Does R_2^* increase or decrease when contrast agent extravasates? A simulation study.

N. Pannetier[1,2], C. Debacker[1,2], F. Mauconduit[1,2], T. Christen[1,3], and E. L. Barbier[1,2]
[1]U836, INSERM, Grenoble, France, [2]Grenoble Institut des Neurosciences, Université Joseph Fourier, Grenoble, France, [3]Department of Radiology, Stanford University, Stanford, California, United States

Introduction: DSC-MRI is a powerful tool to characterize tumor microvasculature and its evolution under therapy. In the brain, quantification of DSC experiments remains a challenge when contrast agent (CA) extravasates into the interstitium as it is the case in many diseases [1]. Indeed, CA extravasation increases R_1 relaxation in the interstitium and causes a signal enhancement. This effect competes with the R_2* increase which lowers the signal and is used in DSC to compute perfusion estimates. Many solutions have been proposed to reduce this R_1-related bias (preload bolus, data truncation or signal modeling, multi-gradient echo sequences). However, the consequences of CA extravasation on R_2* are often overlooked: CA extravasation reduces the magnetic susceptibility difference ($\Delta\chi$) at the intra-/extravascular interface (effect denoted $R_2{}^*_{vasc}$) and CA extravasation yields to the emergence of magnetic susceptibility differences at the interfaces between cells and interstitium (effect denoted $R_2{}^*_{inter}$). In this study, we evaluated these two competing R_2* effects in case of blood-brain barrier (BBB) permeability using numerical simulations for various porosities and cell sizes.

Materials and Methods: We simulated a DSC experiment: a Gd-chelate arrives via the vessel in an elementary volume (considered here as a 2D object), extravasates through the vessel walls and diffuses into the interstitium but remains outside the cells. Thus the interstitium concentration of CA increases with time. The mean concentration of CA in the interstitial space is denoted C_i.

Geometry: *S*imulations take place in a 2D geometry (surface area $S_{tot} = 68^2$ µm^2, described by 580^2 pixels). Vessels (n = 5, surface fraction = 3.6 %) are randomly distributed into the geometry. Circular cells are randomly distributed between vessels and replicated on the borders (*cf.* FIG. 1E). The upper bound for cell radius is set to R_0^{max}. The surface area occupied by vessels and cells is denoted S_{cell}. The tissue porosity, Π, is defined by $\Pi = 1 - S_{cell}/S_{tot}$ and is expressed in percent.

Simulation: CA extravasation and diffusion are simulated during 4 minutes. At t = 0, CA concentration in vessels (C_p) is set to 2 mM and remains constant all along the simulation. At each time step δt (1.3 ms), CA exchange occurs pixel wise between the vessel and the one-pixel-wide vessel periphery (pixel at the vessel periphery are indexed d in the equation). This exchange is described by equation (1) [2]. In the interstitium and for each δt, CA d*iffusion* is modeled using a convolution kernel D_{xy} described by equation (2) [3]. D_{Gd} is the free diffusion coefficient of the Gd ($D_{Gd} = 48.10^{-11}$ m^2.s^{-1},[4]). Convolution is achieved in the Fourier space (for speed and useful aliasing property which ensures mass conservation). Special attention is paid to modeling "rebounds" of Gd on cell and vessel membranes. *Magnetic field* perturbations ΔB (FIG. 1B) are computed at $B_0 = 4.7$ T with the approach based on the Fourier transform of the susceptibility matrix $\chi = \chi_m.C$, where χ_m is the CA molar susceptibility ($0.027.10^{-6}$ mM^{-1} [5]) and C the CA concentration matrix (i.e. the concentration for each pixel of the geometry, FIG. 1A). This approach is summarized by equation (3) [6,7]. Finally, we compute the standard deviation of the magnetic field perturbations over the geometry, $\sigma(\Delta B)$. We used $\sigma(\Delta B)$ as a global evaluation of R_2* in the whole geometry.

Extravasation of CA across the BBB	*Diffusion of CA in the interstitium*	*Magnetic Field*
$\delta C_d(t) = k_{pe}\left(C_p - C_d(t)\right)\delta t$ (1)	$D_{xy} = \left(\frac{1}{4\pi D_{Gd}\delta t}\right)\exp\frac{\left(x^2+y^2\right)}{4D_{Gd}\delta t}$ (2)	$\Delta B = TF^{-1}\left\{B_0\left(\frac{1}{3} - \frac{k_y^2\sin^2\theta}{k_x^2+k_y^2}\right)TF\{\chi\}\right\}$ (3)
with k_{pe} the transfer coefficient across intra-/extravasuclar compartments		with θ the angle between B_0 and the capillaries axis.

Two simulations are conducted. In ***Simulation 1***, R_0^{max} is set to 10 µm and Π varies from 96.4% (no cells) to 20.5% (physiological Π of healthy tissue is about 20%). Three vessel arrangements are simulated. In ***Simulation 2***, Π is set to about 30 % and R_0^{max} varies from 4 µm to 20 µm (*cf.* FIG. 2A).

Results: *Simulation 1 - FIG. 1*. The porosity impacts strongly σ(ΔB) (FIG. 1C). Without cells (Π = 96.4%), σ(ΔB) decreases as C_i increases. With cells, we observe an inflection point in the σ(ΔB) changes for a concentration denoted C_{ip}. C_{ip} is thus the concentration for which the increasing $R_2{}^*_{inter}$ takes over the decreasing $R_2{}^*_{vasc}$. This point is reached at lower C_i as Π decreases (FIG. 1D). For healthy Π, this inflection occurs for $0 < C_{ip} < 0.1$ mM. Note that the maximum of σ(ΔB) does not correspond to the smallest Π (20.5%), where cell interfaces length is however the highest.

Simulation 2 - FIG. 2. At $\Pi \sim 30\%$, cell radius and σ(ΔB) seems to be independent (FIG. 2B). This suggests that the link between the length of cell/interstitium interfaces and the σ(ΔB) is not straightforward.

Discussion/Conclusion: In presence of CA, the cell/interstitium interfaces yields magnetic field heterogeneities. For a healthy Π, σ(ΔB) first decreases then increases as the interstitial CA concentration increases beyond 0.1 mM. Since interstitial CA concentration may reach 1 mM [8] in brain tumors, the contribution of $R_2{}^*_{inter}$ might overcome that of $R_2{}^*_{vasc}$. The key factor for determining the role of each contribution appears to be the porosity rather than the cell radius. Since porosity may be affected in tumor, it is likely that the balance between the two contributions is tumor dependent. This approach could be used to characterize tumor porosity. Furthermore, this phenomenon also applies to dynamic contrast enhanced methods and to all organs where a CA may extravasate.

References: [1] S. Heiland et *al.* J Clin Oncol, 2010. [2] P. S. Tofts. JMRI, 1997 [3] L. M. Klassen et *al.* Biophys J, 2007. [4] B. Marty. ISMRM 2010. [5] R.M.Weiskoff et *al.*, MRM 19992 [6] K. M. Koch et *al.* Phys Med Biol, 2006. [7] J. P. Marques et al. Concept Mag Res B. 2005. [8] M. Beaumont et *al.* JCBFM 2009.

FIGURE 1

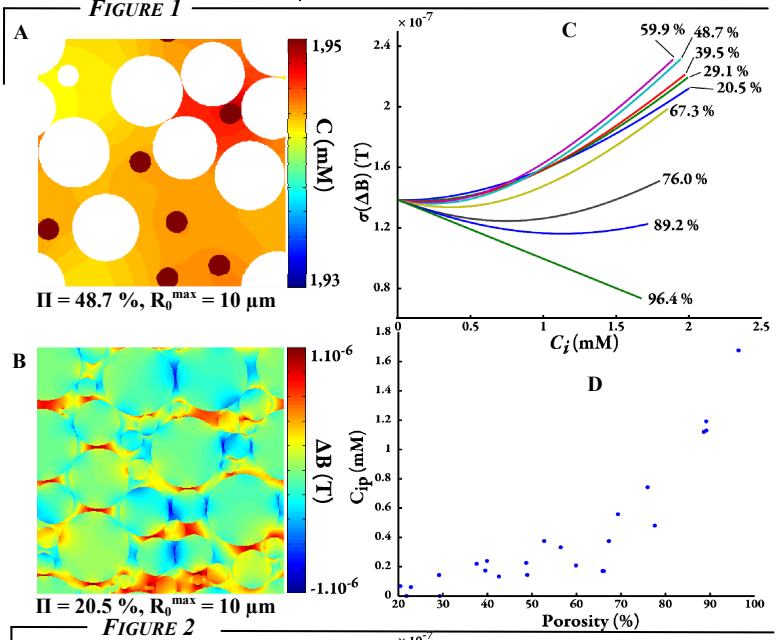

FIGURE 2

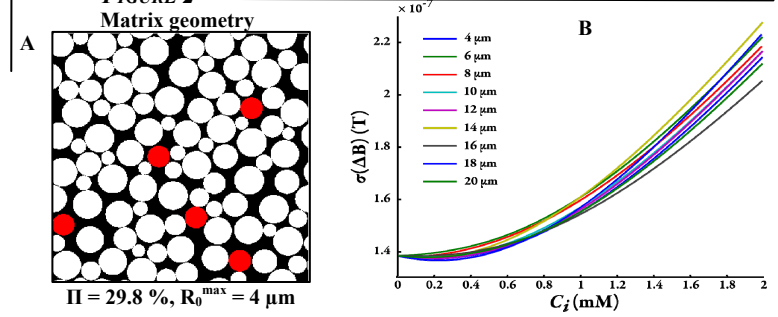

FIGURE 1 – *Simulation 1*. (A) CA concentration matrix for Π= 48.7%, R_0max= 10 µm at t = 4 min. **(B)** Magnetic field perturbations matrix ΔB for Π= 20.5%, R_0max= 10 µm at t = 4 min. **(C)** $\sigma(\Delta B)$ *vs* C_i for 9 different Π values (one colour per Π value). **(D)** Concentration C_i at which the inflection point is reached (C_{ip}) *vs* porosity (3 simulations for 3 geometries).

FIGURE 2 – *Simulation 2*. (A) Example of a matrix geometry with Π= 29.8% and R_0^{max}= 4 µm (white = cells, red = vessels). **(B)** $\sigma(\Delta B)$ *vs* c_i for 9 R_0^{max}